MLS Observations of Atmospheric Gravity Waves over Antarctica

Dong L. Wu and Jonathan H. Jiang

Jet Propulsion Laboratory, California Institute of Technology, Pasadena, California

Keywords: Gravity Waves, Antarctica, Polar Stratospheric Cloud, Circulation, Ozone Depletion

Submitted to: Journal of Geophysical Research - Atmospheres

Date: March 29, 2002

Abstract

This paper presents three years of stratospheric gravity wave observations over Antarctica based on Upper Atmosphere Research Satellite Microwave Limb Sounder (UARS MLS) radiance fluctuations. Strong gravity wave activities are found over the Drake region during August and September each year, where the wave feature is apparently associated with the topography of the South America and the Antarctic Peninsula tips. During the same period, enhanced gravity wave activity is also evident (but to less extent) along the coastal region around Antarctica. The growth of the gravity-wave variance with height shows a scale height of ~14km at low altitudes for both Drake and coastal regions but slows down significantly at high altitudes. The characteristic altitude of the growth slowdown is lower for the stronger variance in the Drake region compared to the weaker variance in the coastal region. In a comparison between MLS gravity-wave distribution and simultaneous polar stratospheric cloud (PSC) observations from CLAES (Cryogenic Limb Array Etalon Spectrometer), we find that the strong gravity wave activity over the Drake region may play a significant role in enhancing PSC formation on the vortex edge. Due to temperature fluctuations induced by gravity waves, more clouds are likely to form in the vicinity of the Drake region even where the synoptic-scale temperature shows 195K or slightly higher.

1. Introduction

Gravity wave (GW) drag has been recognized as one of the essential forcings that control the transport circulation and thermal structure in the middle atmosphere. The scales of most GWs are too small to be resolved by general circulation models (GCMs), and parameterized GW drag is needed for the models to reproduce observed features in the atmosphere. Without the small-scale wave forcing, the stratospheric polar vortices would be too strong and the polar temperature in the upper stratosphere would be too cold [Hamilton et al., 1994; Pawson et al., 2000; Shepherd, 2000]. In the lower atmosphere, including appropriate GW drag parameterizations has been shown to help improve model score of forecasting [Milton and Wilson, 1996]. However, more studies are still needed for better understanding of wave dynamics and sources as well as adequate GW parameterization.

GWs also play a considerable role in the polar ozone depletion by assisting polar stratospheric cloud (PSC) formation [Carslaw et al., 1998]. PSCs have been thought as a key agent in the polar vortex that helps efficiently destroy ozone via heterogeneous reactions. Cariolle et al. [1989] reported a PSC event over Antarctica in early September while severe ozone depletion occurred in the region. The event started with some short-scale features over the Antarctic Peninsula and quickly (within 30 hours) spread to a synoptic-scale area inside the vortex. Although PSC formation has been attributed to both GWs [Carslaw et al., 1998] and synoptic-scale tropospheric forcing [Teitelbaum et al., 2001], the cloud appear near the vortex edge is critical to ozone loss due to early exposure to sunlight. Lee et al. [2001] recognized the importance of ozone loss in the vortex-edge region and argued that more PSC appearance on the edge due to stratospheric cooling could cause a delayed ozone recovery.

Antarctica is unique for its strong nearly axisymmetric flow in the wintertime stratosphere with fewer orographic gravity wave sources compared to the Arctic region. Antarctic circulation produces mean sinking motion throughout the troposphere in the interior of the continent and ascent motion near the coastline. Large elevation changes (2 km in 100-200km) along the coastal region provide most of orographic sources for the GWs around Antarctica. The Antarctic Peninsula stretches out north from the Antarctic continent for 800 miles. It is separated from South America by the Scotia Sea and the Drake Passage, a 0.4-km channel of water connecting the South Atlantic Ocean with the South Pacific Ocean. Rugged offshore islands and glaciers crowd in the Peninsula with a long and narrow land on which mountains rise to 1-2 km. Exposure to open-water winds, which is often stronger than those near the coastline, the tips of the Peninsula and the South American can be very effective orographical sources for GW generation [Bacmeister, 1993].

Observations remain limited comparing to what needed to understand the sources and mechanisms of GW generation due to complex nature of the wave dynamics Especially, validation and constraint of GW forcing in GCMs require global observations of GW activity. In the lower atmosphere GW observations over Antarctica are mainly provided by radiosondes [Allen and Vincent, 1995; Pfennigner, et al., 1999; Yoshiki and Sato, 2000]. However, little study has been given to global morphology of GWs in the troposphere. For the stratospheric observations, Wu and Waters [1996] analyzed gravity-wave-scale radiance fluctuations measured by Upper Atmosphere Research Satellite

Microwave Limb Sounder (UARS MLS) and found good correlation between stratospheric GW activity and the background winds in the Southern Hemisphere (SH) during the winter months. Such correlation is thought mostly due to effects of the background winds on GW propagation [Alexander, 1998]. Jiang et al. [2002] examined the MLS data over Mt. Andes and realized that orographic GWs are detectable with MLS-like instrument even though their amplitudes are weak. In their study, they also identified much stronger wave activity over the Drake region that is apparently associated with the topography around the tips of the South America and the Antarctic Peninsula.

In this paper we present further observational studies with the MLS GW measurements over the Drake region as well as elsewhere over Antarctica. Our observations are focused on three years of MLS limb-scan data in August of 1992-1994 when the stratospheric polar vortex and GW enhancement are strong. The paper is organized to give description of the data and analysis methods in section 2, observational results in section 3, and discussion and conclusion in the end.

2. Data Analysis

The data used in this study are the mesoscale radiance variances of MLS 63-GHz O_2 measurements. Similar to the approach used by Wu and Waters [1996], the variances are computed from the saturated radiance measurements at the bottom of each limb scan. Instead of using six saturated measurements, we use three in this study so that all the radiances, especially those from the outmost wing channels, are sufficiently saturated for the variance analysis. The calculated radiance variance contains an instrument component and an atmospheric component. Since the saturated microwave radiance is a good measure of atmospheric temperature over the saturation layer, the atmospheric variances can be reported as air temperature fluctuations at the layer. For the 63-GHz radiometer there are 15 channels (symmetric about channel 8) that feature 8 altitude layers at about 28, 33, 38, 43, 48, 53, 61, and 80km. Due to MLS antenna field-of-view smearing, these variances are only sensitive to GWs of vertical scales greater than ~10km for channels 1-7 and 9-15 (~15km for channel 8). In addition, the three-point truncation on the radiances limits the horizontal scales to less than ~45km for 2-second integration time on each measurement and a 7.5km/s satellite velocity. Although the restrictions on horizontal and vertical wavelengths yield very small wave amplitudes for MLS to detect, the wave variances are measurable in light of the low instrument noise and stable operation performance.

For the saturated radiances, MLS weighting functions are tilted with respect to the horizon, which gives the instrument significant sensitivity to GW propagation direction [Wu and Waters, 1997; McLandress et al., 2000]. Because of different viewing angles from the ascending and descending orbits, it is necessary to apply the variance analysis separately for these orbits such that the GW variances come out of the same viewing geometry at a given latitude. This is very important when comparing the GW variances observed in different time and longitude. UARS MLS daily latitude coverage is biased between 34° in one hemisphere to 80° in the other because the instrument views 90° from the satellite moving direction. UARS makes 10 yaw maneuvers each year allowing alternating views of high latitudes in the two hemispheres. MLS radiance variance data are available for the period between September 1991 and June 1997. However, only the data in 1992-1994 are used in this study when MLS maintained the same scan scheme (i.e., from top to bottom). Since 1995 MLS changed the scan order to a bottom-to-top operation and introduced a so-called limb-track mode where the antenna did not scan at all and put the pointing at a fixed tangent height. The different scan order alters sampling footprints of the saturated radiance and the limb-track operation reduces the number of scan days in a given month, which altogether make the variances in 1995-1997 complex to compare to the observations in 1991-1994.

3. Results

Figure 1 show the maps of MLS GW activity observed during August of 1992-1994. Despite variability in the amplitude and distribution of GW variances, the salient feature over the Drake region appears to be consistent from year to year. The variances at ~28km are higher in 1992 and 1994 than in 1993 but the year-to-year differences are less prominent at altitudes greater than ~43km. The peak variance over the Drake region is associated more closely to the tip of the South America at ~28km. As height increases, the center shifts slightly towards the Antarctic Peninsula and spreads over a larger area. Contrast of the Drake feature to the surrounding wave activity also reduces at higher altitudes as the growth of the surrounding GWs outpaces one over the Drake region. The variances from the descending orbits (not shown) exhibit similar patterns but the amplitudes are smaller, as expected if most of these GWs are propagating westward in the stratosphere relative to the eastward background winds.

Elsewhere, the GW activity follows the Antarctic coastline quite well, especially at the lowest altitude, with several peaks located along longitudes between 90°-220°. Unlike the feature over the Drake region, the locations of these peaks vary from year to year but are generally correlated between low and high altitudes. In 1992 and 1993 the GW activity at longitudes between 90°-220° appears higher than other coastal regions at

43km. In 1994 the coastal pattern at 43km changes somewhat to exhibit variance enhancement over a larger area at longitudes between 45° and 270°. As found in early MLS variance observations [Wu and Waters, 1996], the enhanced coastal variances reside in the vortex-edge region in the stratosphere and show generally good correlation with the stratospheric jetstream. However, the modulation of the GW variance around the vortex edge cannot be explained by the influence of the stratospheric jetstream.

To study temporal and height variations of GW activity over the Drake region, we define the region as an area between 290°-315° in longitude and 50°S-70°S in latitude and average all the variances in the region on a daily basis. Figure 2 shows the time series of daily GW variances over the Drake region from only the ascending orbits. As the instrument viewed SH high latitudes, there are typically 4-7 measurements falling into the special region each day for the ascending orbits. The low statistics apparently cause large fluctuations in the daily variances. A 21-day running mean, therefore, is applied to the daily averages, which is represented by the smoothed curve superimposed on the time series. Throughout the stratosphere, the GW variance variations over the Drake region are dominated by the annual cycle with the peak activity in August and September. During January-March, wave activity is so low that the variance is not significantly distinguishable from the instrument noise. The year-to-year variability is evident in low-altitude channels but becomes less significant at higher altitudes.

Figure 3 summarizes the variance growth with height over Antarctica during August where the variances are grouped into the Drake and coastal regions. The coastal region is defined as 0°-215° in longitude and 50°S-70°S in latitude, and the variances are normalized by the saturated radiance at each altitude. Both ascending and descending variances reveal a similar growth trend between 28 and 61km showing an exponential increase in amplitude. Characterized by scale height, the growth rate varies with altitude. For the Drake region, the scale height is close to 14km below ~43km whereas it gradually increases at altitudes above that as the variance growth slows down. On the other hand, the variances in the coastal region, starting with a much weaker amplitude, show the same scale height (~14km) up to 53km before the slowdown occurs. This is interesting because the slowdown altitude moves to a higher level for the variances that start with a smaller value at low altitudes.

4. Discussions and Conclusions

Mesoscale radiance fluctuations observed with MLS have been used to infer GW activity over Antarctica although the derived variances are limited to waves of long (>10km) vertical and short (<45km) horizontal scales. Because GW activity often consists of a broad spectrum of wave components, MLS variances are not suitable for deriving total potential energy of the GW package. However, from the spectral portion where MLS is sensitive, we can obtain important information on GW distribution and possible wave sources. The Drake region has been identified as a unique source of GW generation during August and September although it is not clear how the GWs seen in the stratosphere is generated. More studies in modeling and observations in the lower atmosphere are needed to clarify the mechanism(s).

Despite unclear causes of the strong GW activity over the Drake region, one would question what are the potential effects of these waves on atmospheric dynamics in the polar region? It is often observed that the center of the stratospheric polar vortex leans off from the pole toward the Drake region. Is the synoptic-scale motion related to the strong

GW activity in the region? For the month of August, we also examined the simultaneous constituent measurements from CLAES (Cryogenic Limb Array Etalon Spectrometer) N_2O and MLS O_3 and HNO_3 (not shown here) to compare synoptic-scale features with the GW activity over the Drake region. The constituent measurements have been found useful to infer information about dynamical as well as chemical processes of synoptic scales [Santee et al., 1995]. Preliminary results reveal that there is an ascent air of synoptic scales near (in the east of) the Drake region, which gives rise to high N_2O, low O_3 and low HNO_3 at 100hPa during August. Moreover, another offline analysis with MLS upper tropospheric H_2O measurement suggests the similar synoptic-scale ascent at 310hPa in the east of Drake region. The H_2O data also indicates a zone of descent air just west of the Drake region. Altogether, these observations suggest some connections between the GW activity and synoptic-scale tropospheric forcing over the Drake region. More work, however, is required to quantify such interactions between synoptic-scale and mesoscale dynamics in the polar region.

It is not clear what determine the variance growth with height over the Drake region as well as other enhanced GWs along the Antarctic coastal region. The observed GW variances show a continuous growth in amplitude with height although the growth rate is not as perfect as expected for free propagating GWs. Most of growing GWs will encounter a breakdown/saturation level eventually as wave amplitudes become too large to remain stable. The slowdown in the growth rates at higher altitudes in both Drake and coastal regions is likely caused by wave saturation/breakdown as the limit is reached.

As for possible GW impacts on PSC formation, MLS GW activity is compared to the PSC distribution observed simultaneously by CLAES in the $780cm^{-1}$ aerosol extinction data [Plate 3(b) in Mergenthaler et al., 1997]. In August and September 1992, the polar vortex was elongated stretching out towards the Antarctic Peninsula, which caused frequent occurrence of PSCs in the region. The PSC distribution was confined mostly poleward from the tip of the Peninsula, which gives a little overlap with the distribution of the strong GW activity if one uses the 28km GW map in Figure 1. However, in the vicinity of the Drake region, a significant fraction of CLAES PSCs occurred at temperatures greater than the 195K rim on the synoptic map, which may likely be the signatures of GW-induced clouds. The 195K contour from synoptic scale analyses is often used as the upper limit of Type I PSC formation [Toon et al., 1986]. In reality, local temperature can fluctuate substantially around the synoptic-scale temperature in the presence of strong GW activity, which allows PSCs to occur even where the synoptic-scale temperature is near or slightly greater than 195K. Together, the simultaneous observations of CLAES PSCs and MLS GW activity near the Drake region provide strong evidence of GW-related PSC formation around the vortex edge [Carslaw et al., 1998]. Unfortunately, CLAES was able to operate for only 18 months during the UARS mission and no comparisons can be drawn for 1993 and 1994. Since the GW activity over the Drake region is strong and repeatable every August and September, it would be interesting to see whether PSCs have tended to form there frequently in other years when temperatures are around 195K.

In conclusion, we find a strong and persistent GW activity over the Drake region that occurs during August and September each year. The GWs generated in the Drake region are able to propagate up to the mesosphere with the growth scale height close to 14km in the stratosphere. The comparison between the simultaneous MLS GW and CLAES PSC observations suggests that the GWs over the Drake region likely play a significant role in PSC formation on the vortex edge.

Acknowledgment

We thank Drs. Stephen Eckermann, Michelle Santee, and Joe Waters for helpful discussions during development of this study. This work was performed at Jet Propulsion Laboratory, California Institute of Technology, under contract with National Aeronautics and Space Administration, and sponsored by NASA.

References:

Alexander, M. J., Interpretations of observed climatological patterns in stratospheric gravity wave variance, *J. Geophys. Res.*, **103**, 8627-8640, 1998.

Allen, S. J., and R. A. Vincent, Gravity wave activity in the lower atmosphere: Seasonal and latitudinal variations, *J. Geophys. Res.*, **100**, 1327-1350, 1995.

Bacmeister, J. T., Mountain-wave drag in the stratosphere and mesosphere inferred from observed winds and a simple mountain-wave parameterization scheme, *J. Atmos. Sci*., **50**, 377-399, 1993.

Cariolle, D., S. Muller, and F. Cayla, Mountain waves, stratospheric clouds, and the ozone depletion over Antarctica, *J. Geophys. Res*., **94**, 11,233-11,240, 1989.

Carslaw, K. S., et al., Increased stratospheric ozone depletion due to mountain-induced atmospheric waves, *Nature*, **391**, 675-678, 1998.

Hamilton, K., R. J. Wilson, J. D. Mahlman, and L. J. Umscheid, Climatology of the SKYHI troposphere-stratosphere-mesosphere general circulation model. *J. Atmos. Sci*., **52**, 5-43, 1994.

Jiang, J. H., D. L. Wu, and S. D. Eckermann, UARS MLS observation of mountain waves over the Andes, *J. Geophys. Res*., in press, 2002.

Lee, A. M., et al., The impact of the mixing properties within the Antarctic stratospheric vortex on ozone loss in spring, *J. Geophys. Res*., **106**, 3202-3211, 2001.

McLandress, C., M. J. Alexander, and D. L. Wu, MLS observations of gravity waves in the stratosphere: A climatology and interpretation. *J. Geophys. Res.,* **105**, 11,947-11,967, 2000.

Mergenthaler, J. L., J. B. Kumer, and A. E. Roche, and S. T. Massie, Distribution of Antarctic polar stratospheric clouds as seen by the CLAES experiment, *J. Geophys. Res*., **102**, 19161-19170, 1997.

Milton, S. F., and C. A. Wilson, The impact of parameterized subgrid-scale orographic forcing on systematic errors in a global NWP model, *Mon. Wea. Rev*., **124**(9), 2023-2045, 1996.

Pawson, S. et al., The GCM-reality intercomparison project for SPARC (GRIPS): scientific issues and initial results. *Bull. Amer. Meteor. Soc*., **81**, 781-796, 2000.

Pfenninger, M., A. Z. Liu, G. C. Papen, and C. S. Gardner, Gravity wave characteristics in the lower atmosphere at South Pole, *J. Geophys. Res*., **104**, 5963-5984, 1999.

Santee, M. L., et al., Interhemispheric differences in polar stratospheric HNO_3, H_2O, ClO, and O_3, Science, 267, 849-852, 1995.

Shepherd, T. G., The middle atmosphere. *J. Atmos. Solar-Terr. Phys.*, **62**, 1587-1601, 2000.

Teitelbaum, H., M. Moustaoui, and M. Fromm, Exploring polar stratospheric cloud and ozone minihole formation: The primary importance of synoptic-scale flow perturbations, *J. Geophys. Res.*, **106**, 28,173-28,188, 2001.

Toon, O. B., P. Hamill, R. P. Turco, and J. Pinco, Condesation of HNO3 and HCL in the winter polar stratosphere, *Geophys. Res. Lett.*, **13**, 1284-1287, 1986.

Yoshiki, M, and K. Sato, A statistical study of gravity waves in the polar regions based on operational radiosonde data, *J. Geophys. Res.*, **105**, 17,995-18011, 2000.

Wu, D. L., and J. W. Waters, Satellite observations of atmospheric variances: A possible indication of gravity waves, *Geophys. Res. Lett.*, **23**, 3631-3634, 1996.

Wu, D. L., and J. W. Waters, Observations of Gravity Waves with the UARS Microwave Limb Sounder, in Gravity Wave Processes and Their Parameterization in Global Climate Models (K. Hamilton, ed.) New York: Springer-Verlag NATO ASI Series, Vol. **50**, pp.404, 1997.

Figure Captions

Figure 1 GW variances as observed with MLS during August of 1992-1994. Only data from ascending orbits are used to make the maps. The bottom row is the variances from channel 1 at ~28km whereas the top row is from channel 4 at ~43km. These monthly maps are made on 10°x5° longitude-latitude grids and no data are at latitudes of 80° poleward. The instrument noise has been removed from the total radiance variance. Latitude grids are labeled at intervals of 20° from the equator.

Figure 2 Time series of channel 1 and 4 variances over the Drake region. The instrument noise is not removed and indicated with the horizontal line. Large gaps are the missing data while MLS viewed the Northern Hemisphere high latitudes.

Figure 3 Vertical growth of the normalized GW variance, $(\Delta T_b / T_b)^2$, over the Drake and coastal regions for ascending and descending orbits. All measurements during August in 1992-1994 are averaged to produce the growth profiles. A reference (14km scale height) is shown as the straight line on the left.

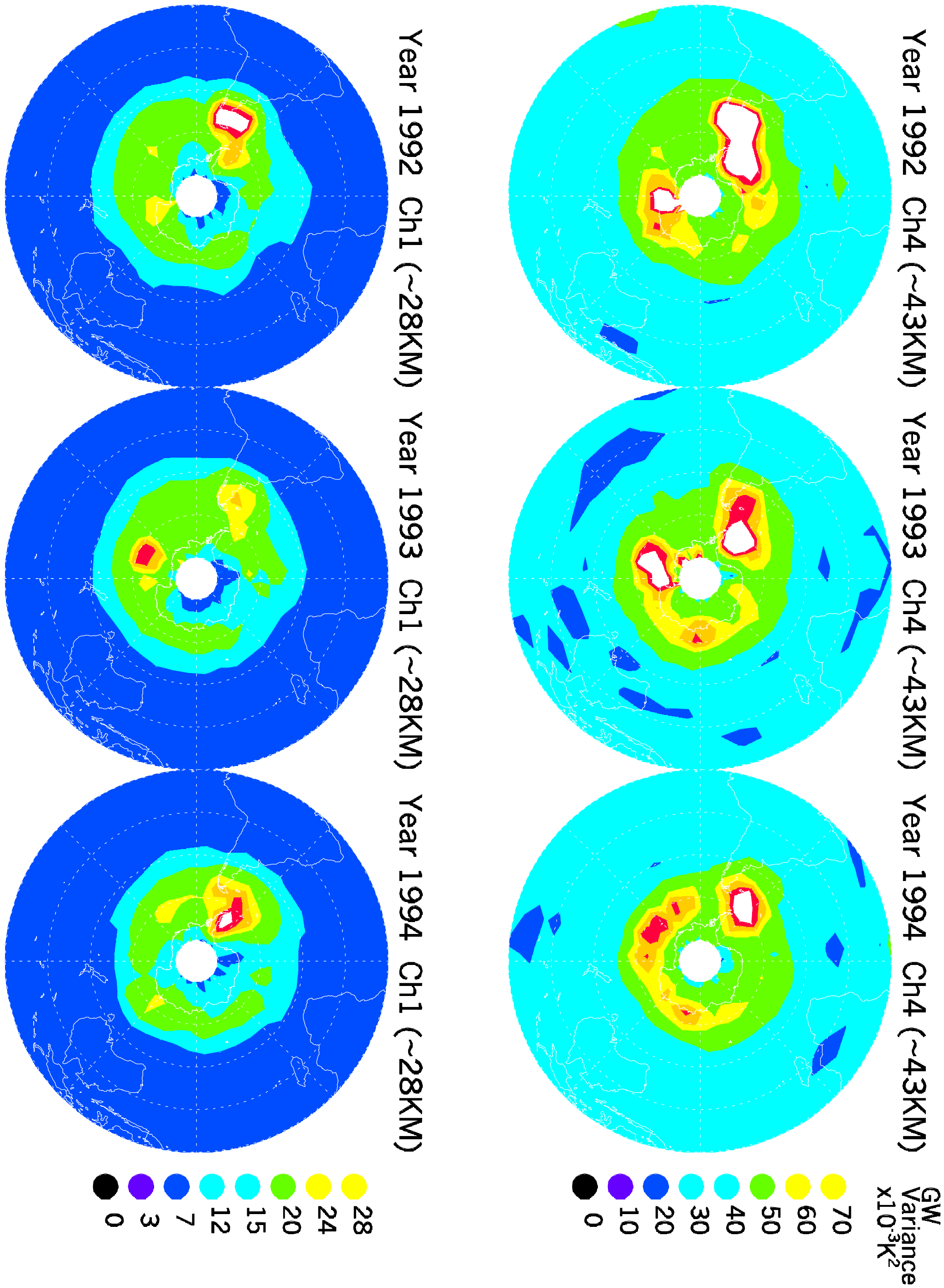

Figure 1 GW variances as observed with MLS during August of 1992-1994. Only data from ascending orbits are used to make the maps. The bottom row is the variances from channel 1 at ~28km whereas the top row is from channel 4 at ~43km. These monthly maps are made on 10°x5° longitude-latitude grids and no data are at latitudes of 80° poleward. The instrument noise has been removed from the total radiance variance. Latitude grids are labeled at intervals of 20° from the equator.

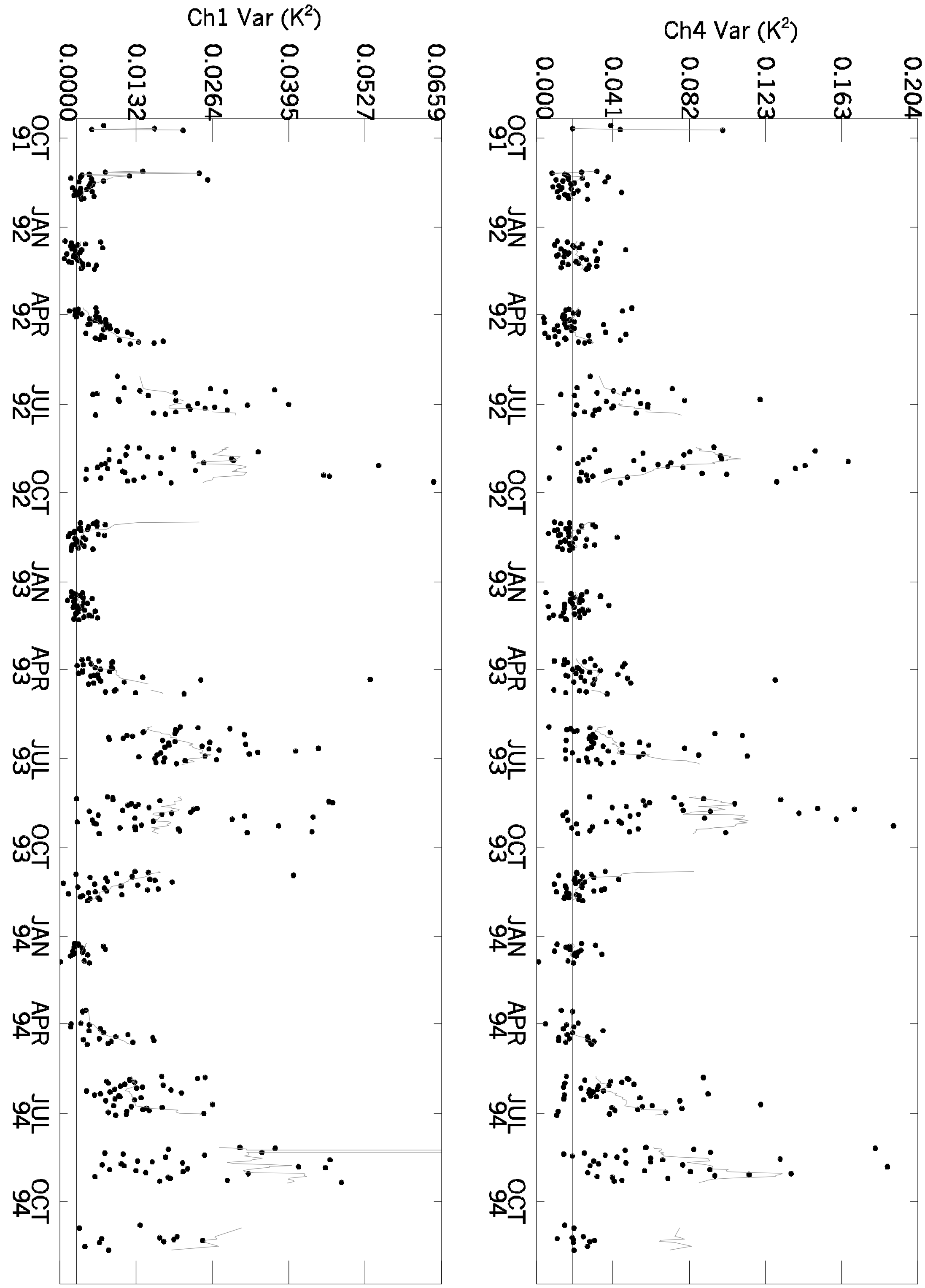

Figure 2 Time series of channel 1 and 4 variances over the Drake region. The instrument noise is not removed and indicated with the horizontal line. Large gaps are the missing data while MLS viewed the Northern Hemisphere high latitudes.

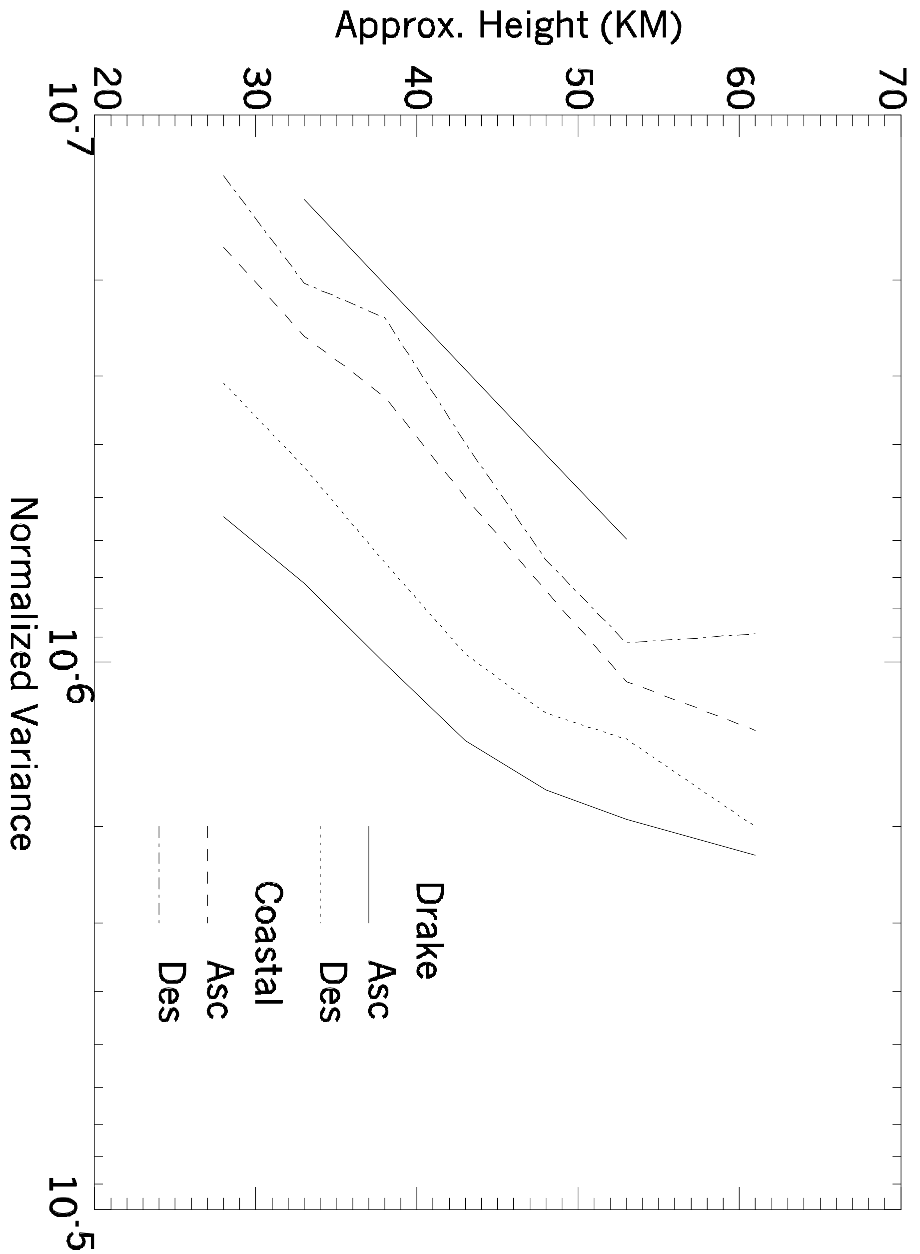

Figure 3 Vertical growth of the normalized GW variance, $(\Delta T_b/T_b)^2$, over the Drake and coastal regions for ascending and descending orbits. All measurements during August in 1992-1994 are averaged to produce the growth profiles. A reference (14km scale height) is shown as the straight line on the left.